Original Article

Safflower-Derived Cationic Lipid Nanoparticles: Potential Impact on the Delivery of SARS-CoV-2 MRNA Transcripts

Shahsavandi, S[1*], Nasr Isfahani, H[2], Hariri, AA[2], Sharifnia, Z[2], Soleimani, S[1], Moradi, A[2]

1. *Razi Vaccine and Serum Research Institute, Agricultural Research Education and Extension Organization, Karaj, Iran.*
2. *Razi Biotechnology Department, Behyaar Sanaat Sepahan Company, Isfahan, Iran.*

ABSTRACT

The COVID-19 pandemic has significantly highlighted the successful application of lipid nanoparticles (LNPs) as an advanced platform for mRNA vaccine delivery. Ionizable lipid is the main component for complexing the mRNA in LNP formulation and *in vivo* delivery. In the first step of this study, we used the native safflower oil seed to prepare dilinoleyl alcohol. Then the cationic lipid DLin-MC3-DMA (MC3) was synthesized by mixing the alcohol with dimethylamino butyric acid. Safflower-derived MC3 was applied to formulate an LNP vector with standard composition. The efficiency of the synthetic cationic lipid was evaluated for delivering an mRNA-based vaccine encoding the receptor-binding domain (RBD) of SARS-CoV-2. The produced mRNA-LNP vaccine candidate was evaluated in size, morphology, mRNA encapsulation efficiency, apparent pKa, and stability for nucleic acid delivery. Cellular uptake was determined by measuring the percentage of GFP expression, and cytotoxicity was assayed using MTT. The MC3 formation was confirmed by the NMR spectra and used as a cationic lipid in LNP formulation. The obtained LNPs had positively charged and appropriate particle sizes (~80 nm) to confer proper encapsulation efficiency for mRNA delivery and stability. The LNPs were shown to be effective in the transfection of mRNA transcripts into HEK293T cells. A high level (72.34%) of cellular uptake was determined by measuring the percentage of GFP expression. The cytotoxicity assay using MTT showed that both LNP and mRNA-LNP were non-toxic to cells. These data demonstrate the potential of the proposed safflower-derived cationic lipid in the formulation of LNP. The carrier provides a promising platform for the efficient delivery of mRNA *in vitro*. Further evaluations of its potential for *in vivo* delivery are needed.

Keywords: Cationic Lipid, Lipid-based Nanoparticles, Safflower oil, RNA vaccine, SARS-CoV-2.

1. Introduction

Lipid-based nanoparticles (LNPs) have constituted a pivotal element in the evolution of vaccine technology, with their origins tracing back to the initial description of liposomes in 1961. In the 1980s, significant advancements were made in the traditional forms of LNPs, resulting in enhanced accumulation at target cells. Subsequent developments resulted in the creation of multi-component formulations that were specifically designed to deliver oligonucleotides to targeted tissues (1, 2). A significant milestone was achieved in 2018 with the advent of siRNA-LNPs (Onpattro®), targeting polyneuropathy in transthyretin-mediated hereditary amyloidosis (3). The recent coronavirus pandemic has brought mRNA-based vaccines into the spotlight, with praise being directed towards them for their stability, safety, and efficacy in eliciting both B and T cell immune responses. The concept of mRNA vaccines, which involves the transfer of genetic information from DNA in the nucleus to the cytoplasm of a cell in the form of mRNA, originated as a theoretical idea in 1961 and was subsequently demonstrated as a practical application in animal models by 1990 (4-6). A pivotal moment in this journey was the successful demonstration by Wolff et al. of mRNA expression in mouse skeletal muscle cells (7). Since then, significant strides have been made in overcoming the inherent limitations of mRNA structures, enhancing their therapeutic potential. These improvements include the incorporation of modified nucleosides, such as N1-methylpseudouridine, to enhance molecular stability; the optimization of mRNA capping modalities and UTR selection for improved translation efficiency and intracellular stability; codon optimization; and the addition of poly(A) sequences to mitigate RNA exonuclease degradation (8-11). Nevertheless, successful formulation and in vivo delivery of mRNA are beset with challenges like high negative charge density and enzymatic instability in biological fluids. Owing the problems, necessitate meticulous optimization to ensure vaccine efficacy, stability, and non-toxicity. LNPs, especially those composed of ionized lipids such as DLin-MC3-DMA (referred to as MC3), PEG-lipids, Distearoylphosphatidylcholine (DSPC), and cholesterol, have been instrumental in this context (12). Ionizable cationic lipids are critical in mRNA-LNP formulation because of the strong electrostatic interaction with the encapsulated RNA. They form electrostatic complexes with negatively charged nucleic acids, enhancing the electric charge of nanoparticle surfaces and facilitating mRNA endocytosis, while also safeguarding the encapsulated mRNA from ribonucleases (13-15). In our study, we focus on the MC3 lipid, notable for its FDA approval in RNA therapies and its efficacy in mRNA-LNP formulations. From a chemical perspective, MC3 contains two C18 linoleic acid tails that contributed to an increase in the transfection efficiency of LNPs. The lipid was synthesized by combination of dilinoleyl alcohol with dimethylamino butyric acid in the presence of 1-Ethyl-3-(3-

dimethylaminopropyl) Carbodiimide Hydrochloride (EDCI.HCl) (16-17). From a chemical perspective, MC3 contains two C18 linoleic acid tails that could increase the transfection efficiency of LNPs. Safflower edible oil is composed a high level of linoleic acids with a mean value of 70.66% (1). We first synthesized MC3 from safflower oil through a multi-step process, then prepared an LNP-encapsulated mRNA of SARS-CoV2. We used the RBD-dimer mRNA according to SARS-CoV-2 Delta (B.1.617.2) and Omicron (B.1.1.529) variants. The particle size polydispersity index, zeta potential, encapsulation efficiency, and *in vitro* cytotoxicity of the mRNA-LNPs were evaluated to ascertain their potential in vaccine applications. In our study, we focus on the MC3 lipid, notable for its FDA approval in RNA therapies and its efficacy in mRNA-LNP formulations. From a chemical perspective, MC3 contains two C18 linoleic acid tails that contributed to an increase in the transfection efficiency of LNPs. The lipid was synthesized by combination of dilinoleyl alcohol with dimethylamino butyric acid in the presence of 1-Ethyl-3-(3-dimethylaminopropyl) Carbodiimide Hydrochloride (EDCI.HCl) (16-17). From a chemical perspective, MC3 contains two C18 linoleic acid tails that could increase the transfection efficiency of LNPs. Safflower edible oil is composed a high level of linoleic acids with a mean value of 70.66% (1). We first synthesized MC3 from safflower oil through a multi-step process, then prepared an LNP-encapsulated mRNA of SARS-CoV2. We used the RBD-dimer mRNA according to SARS-CoV-2 Delta (B.1.617.2) and Omicron (B.1.1.529) variants. The particle size polydispersity index, zeta potential, encapsulation efficiency, and *in vitro* cytotoxicity of the mRNA-LNPs were evaluated to ascertain their potential in vaccine applications.

2. Materials and Methods

2.1. Extraction and Purification of Safflower Oil

Safflower (*Carthamus tinctorius* L.,) is an annual crop belonging to the Asteraceae family; native to the Middle East, parts of Asia and Africa. Safflower seeds were provided from the National Agricultural Research Institute, Isfahan, Iran. The seeds were ground into powder and subjected to hexane extraction in a Soxhlet apparatus (Juhaimi FA, Uslu N). The extracted oil was then purified through a series of steps: degumming with water and phosphoric acid, bleaching with hydrated aluminum silicate, and final refinement.

2.2. Preparation of Linoleyl Alcohol

Fatty acids, including oleic, linoleic, and linolenic acids, were isolated from the safflower oil triglycerides through saponification (Figure 1). This process involved heating 1.25 L of glycerin with 200 g of potassium hydroxide until dissolution, followed by the addition of 500 ml of heated safflower oil. The mixture was stirred at 100°C and treated with 750 ml of 25% sulfuric acid and 1 L of hot water until the oil phase clarified. The aqueous phase was then discarded, and the oil phase was washed and heated to 130°C. The composition of the fatty acids and functional
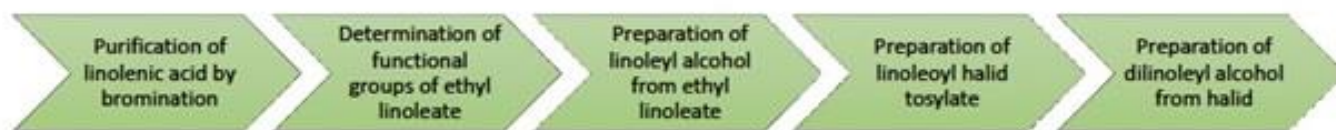
Figure 1. Flowchart of dilinoleyl alcohol synthesis from linolenic acid

groups was analyzed using Gas Chromatography-Mass Spectrometry (GC-MS) and Fourier Transform Infrared Spectroscopy (FTIR).

2.3. Synthesis of Dimethylamino Butyric Acid

Dimethylamino butyric acid salt was synthesized from a mixture of 1.98 g N-methyl-2-pyrrolidone, 12 ml of distilled water, and 2.3 ml sodium hydroxide. The mixture was refluxed for 10 hours at a pH adjusted to 8 using 10% HCl. After solvent evaporation, 6 ml of formic acid and 5 ml of formalin were added, and the mixture was refluxed for an additional 8 hours. Upon completion, 3 ml of HCl was added, the solvent was evaporated, and the product was washed with acetic acid. The functional groups of the synthesized dimethylamino butyric acid were identified using FTIR.

2.4. Formation of MC3

To form MC3 ($C_{43}H_{79}NO_2$), 144 grams of the synthesized dilinoleyl alcohol were dissolved in 1 liter of dichloromethane. Subsequently, 55 g of dimethylamino butyric acid salt, 70 mL of diisopropyl ethylamine, and 4 g of dimethylaminopyridine were added and stirred for a period of five minutes at room temperature. Subsequently, 80 g of EDCI.HCl was introduced, and the reaction mixture was stirred for 24 hours at room temperature. The resulting mixture was diluted with 500 mL of dichloromethane and subjected to sequential washing with saturated sodium carbonate, water, saturated saltwater solution, and drying over sodium sulfate. The prepared MC3 was subjected to nuclear magnetic resonance (NMR) spectroscopy analysis.

2.5. RBD Plasmid and *In Vitro* mRNA Transcription

2.5.1. Gene Synthesis and Cloning

The gene sequence encoding the heterodimeric receptor binding domain (RBD) of the SARS-CoV-2 Delta and Omicron variants (Accession No. PP084047) (19) was synthesized and subsequently cloned into the pVAX1 expression vector (Invitrogen™, Cat# V26020). This vector was selected for itscapability to produce functional mRNA, which contains a T7 RNA polymerase-recognized upstream promoter, the eGFP reporter gene bordered by 5' UTR, cDNA encoding the RBD dimer, 3' UTR, a poly (A) tail, and restriction sites for *Eco*RI and *Bgl*II enzymes.

2.5.2. *In Vitro* Transcription (IVT)

Linearized plasmid DNA was subjected to IVT using the T7 ULTRA Transcription Kit (Invitrogen™, Cat# AM1345), according to the manufacturer's instructions. This process resulted in the generation of the capped and tailed mRNA, which was subsequently purified using the GenElute™ mRNA Miniprep Kit (Invitrogen™, Cat# K0503). The integrity of mRNA was determined using an agarose gel containing the nucleic acid binding dye during

the IVT reaction procedure. The mRNA samples were kept in RNA*later* Stabilization Solution (Invitrogen™, Cat# AM7020) and run on 2% agarose gel containing GelRed™ Nucleic Acid Gel Stain (Biotium, Cat# 41003) at 120 V for 1 h using the ssRNA ladder (New England Biolabs, Cat# N0362S). The purified mRNA concentration was measured by Nanodrop 2000c (Thermo Fisher Scientific). Purified mRNA was kept at -70°C until further use.

2.6. mRNA-LNP Preparation

A lipid-ethanol cocktail for the LNPs was prepared with a total lipid concentration of 50 mM, comprising the synthesized MC3, 1,2-distearoyl-sn-glycero-3-phosphocholine (DSPC; Cat# 850365P), cholesterol (Cat# C8667), and DMG-PEG2000 (Cat# 880151P). Each lipid was dissolved in ethanol to achieve molar ratios of 50:10:38.5:1.5. Concurrently, the purified RBD dimer mRNA was dissolved in 25 mM sodium citrate buffer (pH=4) and injected gently under vigorous shaking into the lipid-ethanol solution corresponding to N:P charge ratio of 4.0. The concentrations and volumes of the components used in LNP preparation are shown in Table 1. The solution was subjected to dialysis against PBS without Ca^{2+} and Mg^{2+} (pH=7.5) for 6 h at 4°C to remove ethanol and un-loaded mRNA. All chemicals were purchased from Sigma-Aldrich.

2.7. mRNA-LNP Characterization

The particle size, zeta potential, encapsulation efficiency, morphology, and stability of the LNPs and mRNA-LNP were carefully evaluated. 100 µL of mRNA-LNPs were diluted in in 900 µL PBS (pH=7.4) for the measurement of the z-average diameter and polydispersity index (PDI) using dynamic light scattering measured on a Malvern Zetasizer Nano-ZS (Malvern Instruments Ltd., UK) following material refractive index of 1.4, absorbance of 0.01, dispersant viscosity of 0.8872 cP, refractive index of 1.330, and dielectric constant of 79 setting at 25°C. The percentage of encapsulated mRNA was determined using the Quant-iT RiboGreen RNA Reagent Kit (Invitrogen™, Cat# R11490). The mRNA-LNP suspension was diluted with 1x TE buffer with and without 0.1% (v/v) Triton X-100 (Sigma Aldrich, Cat# T8787), vortexed briefly, and incubated for 10 min at 37°C to release the encapsulated mRNA. The samples were incubated with Ribogreen reagent at 37 °C for 15 min. Then fluorescence of pre-lysis and post-lysis of LNPs was measured at Ex: 485/Em: 530 nm to determine the encapsulation efficiency percent (EE%) by % EE=(lysed LNP − not lysed LNP)/lysed LNP×100 equation. Morphology of the dialyzed mRNA-LNPs was detected by transmission electron microscope

Table 1. The formulation scheme for mRNA-LNP preparation

	Component	Concentration (mg/ml)	Volume (µl)
Ethanolic phase	MC3	1	12.5
	DSPC	0.5	16.9
	Cholesterol	1	3.1
	DMG-PEG2000	0.5	13.6
	Ethanol	-	125
Aqueous phase	mRNA	1	2.5
	Citrate buffer	-	122.5
	PBS	-	250

(TEM) (Zeiss-EM10C-100 KV, Germany). The LNP sample film was stained with a solution of 2% uranyl acetate and visualized using an acceleration voltage of 80 kV.

2.8. Surface Acid Dissociation Constant (pKa) Measurement

The pKa of the LNPs was assessed using the 2-(p-toluidinyl) naphthalene-6-sulfonic acid (TNS) assay in a 96-well microplate. Buffered solution of 10 mM HEPES (Cat# H4034), 130 mM NaCl, 10 mM NH4OAc, 10 mM MES (Cat# 69889) was titrated to pH values ranging from 3.0 to 10.0 with 0.5 pH unit increments. Then 186 µl of the buffer was mixed with 12 µl of the LNP solution (0.5 mM total lipid) and 2 µl of TNS (Cat# 195243) for a final concentration of 20 µM of LNP and 6 µM of TNS in each well. The fluorescence intensity of the TNS was quantified at Ex: 321/Em: 445 nm. The pKa was determined as the pH value corresponding to 50% LNP protonation at 50% of maximal fluorescence intensity. The chemicals were purchased from Sigma-Aldrich.

2.9. Stability of mRNA-LNP

Samples of the mRNA-LNPs were stored at 4 °C and checked for stability by analyzing the particle size, DPI, zeta potential, and encapsulation rate changes at one-week intervals until 4 weeks.

2.10. *In Vitro* mRNA Transfection

Human embryonic kidney (HEK) 293T cells were maintained in complete Dulbecco's Modified Eagle's Medium (cDMEM; Gibco[TM]) supplemented with 10% FBS (Gibco[TM]) and 1% penicillin/streptomycin solution (Gibco[TM]) at 37 °C in a humidified atmosphere containing 5% CO_2. Using the transfection reagent Lipofectamine 2000 (Thermo Fisher Scientific), mRNA was transfected into the cells according to the manufacturer's instruction. The transfection mixture was prepared by the addition of 2 µl Lipofectamine 2000 and 1.5 µg mRNA to 500 µl Opti-MEM I reduced serum media (Gibco[TM]) and incubation for 15 min at room temperature. Cells were seeded at 3×10^5 concentration per well of a 6-well plate. The transfection complexes were added to the cells and incubated at 37°C and 5% CO_2 for 4 h, then the medium was replaced with cDMEM. Cells were harvested 48 h after transfection and

examined for transfection efficiency using BD Accuri™ C6 Plus flow cytometer at the excitation/emission wavelengths of 488/533 nm and 488/585 nm, respectively.

2.11. Cellular Uptake and Cytotoxicity Measurements

In parallel, the mRNA-LNPs at a final mRNA concentration of 1.25 ng/µl were directly inoculated to HEK293T cells cultured in cDMEM containing FBS and antibiotic solution, and incubated at the same conditions. After 12, 24, 48 h of transfection, cells were washed three times with PBS to remove non-internalized particles, then resuspended in 250 µl of fresh cDMEM. The mRNA-LNP uptake was determined by measuring the percentage of GFP expression using flow cytometry. Cytotoxicity following mRNA-LNP transfection was assayed using MTT (3-(4,5-dimethylthiazol-2-yl)-2,5-diphenyltetrazolium bromide) assay. Briefly, HEK293T cells were cultured into 96-well microplate at a concentration of 1×10^4 cells/well and allowed to attach for 24 h. The cells were transfected with mRNA-LNP for 72 h. After washing the cells, MTT (Sigma-Aldrich, Cat# M5655) solution at a final concentration of 5 mg/ml was added to each well. Cells were incubated for an additional 4 h then absorbance was measured at 570 nm. The experiment was done in duplicates. The percentage of cell viability was determined by dividing the absorbance of the transfected cells by the average absorbance of mock cells.

2.12. Statistical Analyses

Statistical analyses of the data were performed using one-way ANOVA and shown as + mean standard deviation (SD). P<0.05 was considered statistically significant. All data are representative of three independent experiments.

3. Results

The GC was used to provide a detailed quantitative analysis of the fatty acid composition of the purified safflower oil. The GC analysis demonstrated a high content of oleic acid and linoleic acid, which collectively formed the majority of the oil's fatty acid profile (Figure 2). The domination of these specific fatty acids in safflower oil emphasizes its suitability as a raw material in the synthesis process. Changes that occurred in functional groups participating in the dilinoleyl alcohol synthesized from linolenic acid and

dimethylaminobutyric acid formation reactions were identified by FTIR. The FTIR spectra revealed significant findings. A broad peak at 3433 cm^-1 attributed to hydroxyl (-OH) groups was prominent in the ricinoleic acid molecule. Additionally, a peak at 1662 cm^-1 indicative of C=C double bond stretching became more pronounced with an increasing mole ratio of methylaminohexane (MAH) in the reaction. This was especially noticeable at a CO:MAH molar ratio of 1:2, suggesting a heightened level of ester group attachment to the safflower oil molecule chains. Notably, the absence of cyclic anhydride peaks at 1779 and 1849 cm^-1 indicated that most of the MAH had reacted with the safflower oil. The MC3 formation is also confirmed by the NMR spectra (Figure 3), which displayed distinct peaks in the carbonyl region: C1 of free fatty acids at 174–176 ppm, C1 in the 1,3-sn position of triacylglycerols at 173.26 ppm, and C1 in the sn-2 position of triacylglycerols at 172.81 ppm. These peaks were crucial in verifying the successful synthesis of MC3, as they specifically matched the expected chemical structures. The mRNA was transcribed from a linearized DNA template followed by capping, poly(A) tailing, and a DNase treatment. Electrophoresis of the mRNA samples on agarose gel confirmed the integrity, size, and presence of the poly(A) tail during the IVT procedure (Figure 4). The concentration of mRNA was estimated 2.88 g/l of IVT reaction. Subsequently, we assessed the suitability of the synthesized MC3 as a cationic lipid in LNP formulations. The size, surface charge, encapsulation efficiency, and pKa of the resultant mRNA-LNPs were evaluated (Figure 5). According to the physical properties data, the mRNA-LNP demonstrated an average hydrodynamic size of 81.716+1.6 nm with a PDI of 0.064+0.030, and the average zeta potential of -5.834+1.518 mV when formulated at N:P ratio of 4. An efficient mRNA encapsulation rate of 68.73% was determined through the Ribogreen assay. The representative TEM image shows the spherically shaped LNPs with a size around 80 nm, in agreement with the DLS results. The pKa value was determined by fluorescence titration of the LNPs from pH 3.0 to 10.0 and found to be around 6.48. The physical stability of the mRNA-LNP was monitored over four weeks, with assessments of size, PDI, zeta potential, and mRNA entrapment detailed in Table 2. The average size and PDI of the mRNA-LNP suspension either slightly increased or remained unchanged. During the first two weeks, the zeta potential and encapsulation efficacy of the mRNA-LNPs were retained and changed after that. Notably, there was an increase in zeta potential at the end of the storage period compared to immediately post-synthesis (week 0). The decrease in EE% suggested a potential loss in mRNA integrity after storage at 4°C. However, these changes in the physicochemical properties of the mRNA-LNPs were not statistically significant (P<0.05). The final phase involved *in vitro* validation of mRNA-LNP delivery into HEK-293T cells compared to Lipofectamine as the gold standard of transfection. Cellular uptake was studied by flow cytometry. The ability of the LNP in the cellular delivery of mRNA was further assayed by determining transfection levels represented by the GFP expression in the cell population. As the positive control, 93.74% of the viable HEK293T cells transfected with mRNA using Lipofectamine 2000 showed GFP expression. The LNPs also exhibited 72.34% delivery of mRNA into the cell line (Figure 6). The expression of the GFP was preserved for 48h. A key point in the success of LNPs in the transfection of mRNA cargo is their safety. The cytotoxic effect of the prepared LNPs was studied for up to 72 h post-transfection and showcased only a non-significant slight decrease in the cell populations (Figure 6). The LNPs exhibited a minor effect on HEK293T cells with over 80% viability indicating low cytotoxicity. By 48 h, exposure of mRNA-LNPs at an N:P charge ratio of 4.0 resulted in low toxicity with cell viability higher than 80%. Similar to the untreated cells, a decline in viability was detected in mRNA-LNP-exposed cells at 72 h, which is a normal process in the cell cycle. Viabilities of the transfected cells showed no significant difference compared with the untreated cells. A key point in the success of LNPs in the transfection of mRNA cargo is their safety. The cytotoxic effect of the prepared LNPs was studied for up to 72 h post-transfection and showcased only a non-significant slight decrease in the cell populations (Figure 6). The LNPs exhibited a minor effect on HEK293T cells with over 80% viability indicating low cytotoxicity. By 48 h, exposure of mRNA-LNPs at an N:P charge ratio of 4.0 resulted in low toxicity with cell viability higher than 80%. Similar to the untreated cells, a decline in viability was detected in mRNA-LNP-exposed cells at 72h, which is a normal process in the cell cycle. Viabilities of the transfected cells showed no significant difference compared with the untreated cells.

4. Discussion

The efficacy of LNPs as a sophisticated delivery platform for mRNA has been extensively documented in the context of the COVID-19 pandemic caused by various variants of SARS-CoV-2 (20). While the transfection efficiency of a variety of RNAs has been successfully achieved, the risk of cytotoxicity and hemotoxicity represents a significant challenge associated with the use of cationic lipids in LNP formulations (21). As an alternative, plant-derived lipids offer a non-toxic profile and the potential to develop effective vaccines and/or therapeutics. Safflower oil contains a high proportion of oleic and linoleic acids, as well as a high stability index, which collectively make it an ideal carrier for use in drug delivery systems (18). In this study, we have focused on the synthesis of a linoleic acid-derived MC3 and used it to generate an LNP with mRNA delivery efficacy. The primary chemical analysis indicates linoleic acid is the major fatty acid in the prepared safflower oil. Linoleic acid is a carboxylic acid with an 18-carbon chain and two cis-double bonds at positions 9 and 12. Ionizable lipids share common structure features comprising the head group responsible for the pKa value
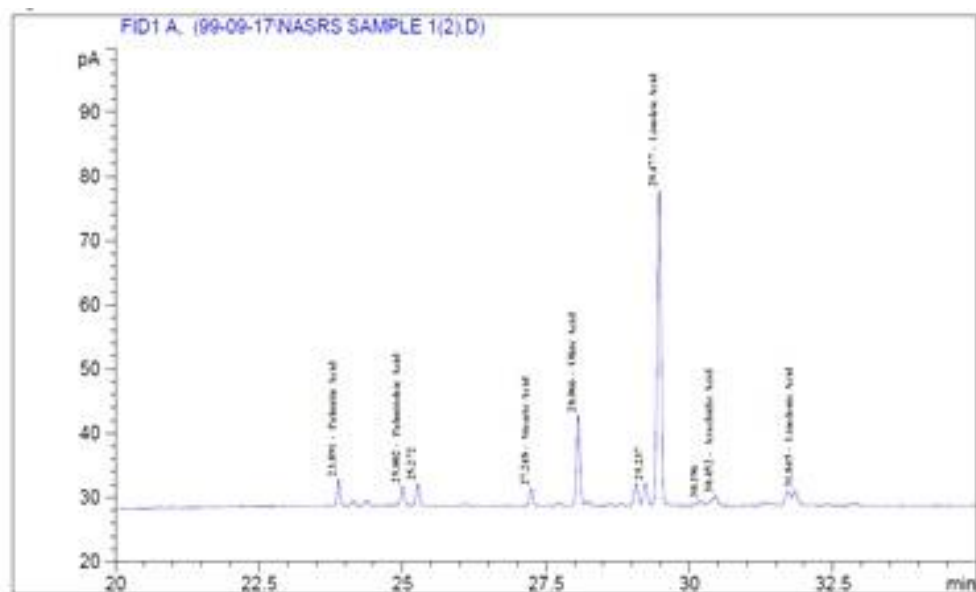
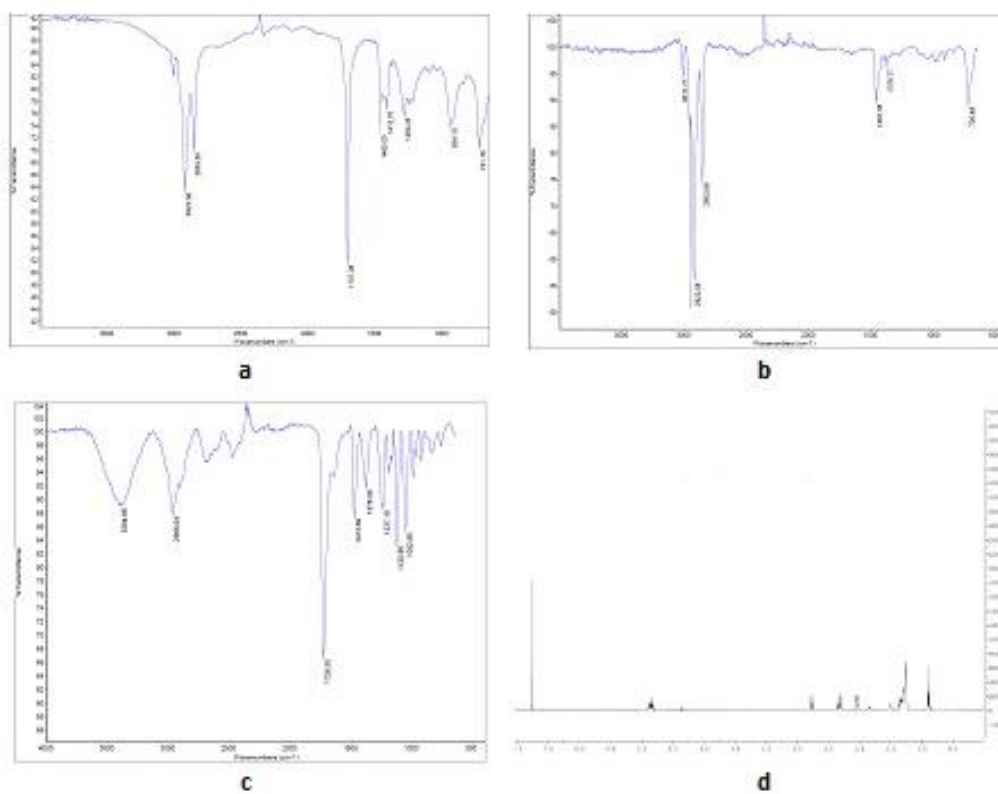**Figure 2.** Fatty acid compositions of the safflower oil using GC-MS

Figure 3. FTIR spectra of (a) linoleic acid, (b) dilinoleyl alcohol, and (c) dimethylaminobutyric acid. (d) ^{1}H NMR spectrum of MC3
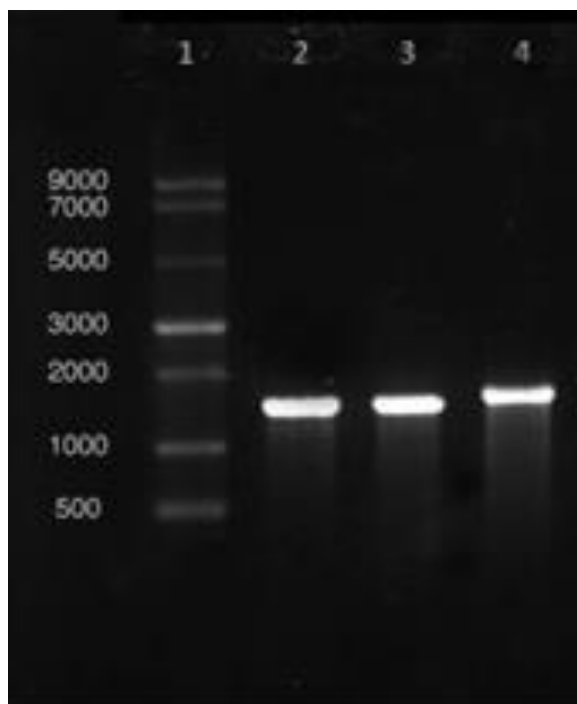
Figure 4. GelRed pre-stained gel shows the integrity of RBD mRNA. Lane 1: RNA size marker; lane 2: mRNA post-IVT; lane 3: mRNA post capping; lane 4: mRNA tailing resulted in a poly (A) tail of about 140 bases.
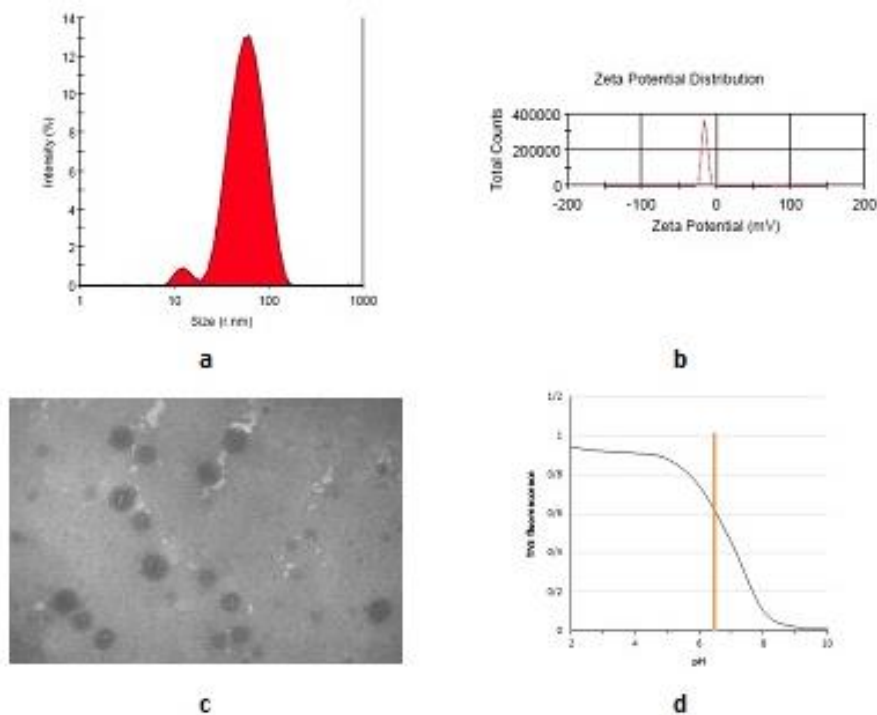

Figure 5. Lipid-based nanoparticle physicochemical characterization: (a) dynamic light scattering data represents hydrodynamic size in the range of 81.72 nm; (b) nanoparticle surface charges in terms of potential analysis shows zeta potential −5.83 mV; (c) TEM image indicates the spherical morphology, (d) TNS assay plot of representative LNPs to determine the apparent pKa.

Table 2. Changes in the physicochemical properties of the mRNA-LNPs during storage period

Storage time (week)	Size	DPI	Zeta potential	EE%
0	81.72	0.074	-5.83	68.73
1	81.62	0.074	-5.27	68.00
2	82.15	0.072	-2.41	66.26
3	83.44	0.070	0.66*	64.14
4	84.83	0.070	7.15*	63.32

Data are the average values of three replicates corresponding to each storage time. The significant difference ($P<0.05$) shown with asterisk.
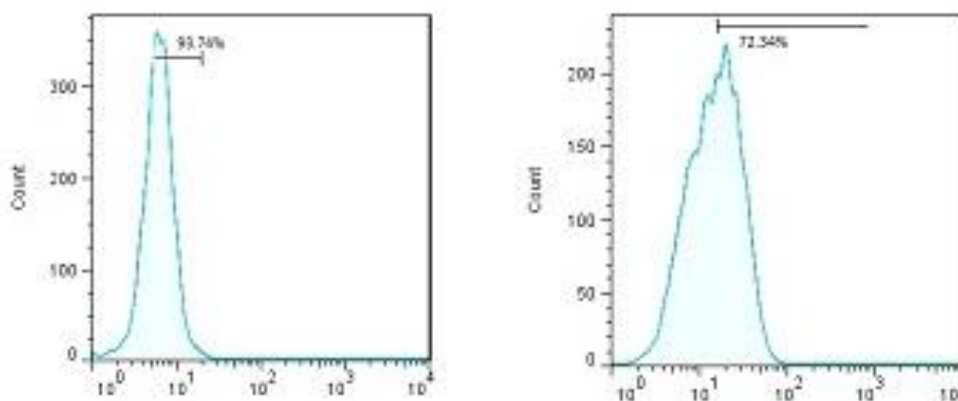

Figure 6. The transfection efficiency of mRNA-LNP in HEK293T cells by flow cytometry. The transfection levels represented as the mean GFP fluorescent signals from 10,000 cells analyzed (left) treated with mRNA-Lipofectamine 2000 and (right) treated with mRNA-LNP.

and charge, ester linker, and linoleyl tail components. Generally, the head group of FDA-approved ionizable lipids is protonated under acidic conditions to facilitate RNA loading into LNPs. The hydrocarbon chains of the head groups are connected through chemically stable ester groups or linkers to improve the biodegradation rate of the lipids after mRNA delivery. Finally, the saturation rate and the cis-double bonds of the tails greatly influence the fluidity and enhance membrane disruption leading to increased efficiency of mRNA delivery (22, 23). The branched tails determine the ability of different cationic lipids to deliver RNA cargo into targeted cells. MC3 contains two linoleic acid-derived tails, each of which includes di-double bonds (22). It has been shown that SM-102 ionized lipid used in Moderna's and ACL-315 used in BioNTech/Pfizer mRNA vaccines have three and four branched tails, respectively corresponding to enhanced mRNA delivery efficiency (24). Subsequently, the MC3 was utilized in the preparation of LNPs with an optimized molar ratio of 50:10:38.5:1.5, followed by an ethanol injection. The LNPs exhibited diameters of 79–85 nm and narrow distributions (PDI < 0.1). A review of the literature on LNP injection indicates that smaller particles are more readily transported from the injection site, resulting in efficient lymphatic drainage and cellular interactions. The

mRNA-LNPs, which are sized between 80 and 100 nm, are preferentially taken up by antigen-presenting cells (APCs), elicit antigen expression, and generate an immune response. The cellular uptake and distribution of mRNA-LNPs are contingent upon the electrostatic interaction between the positively charged head of the ionizable lipid and the negatively charged mRNA (25). Moreover, the branched tail of the lipid may facilitate mRNA release to the cytosol (22, 23). In this study, the mRNA-LNPs exhibited a lower zeta potential than the unloaded LNP, which can be attributed to the negative charge of the mRNA and the strong electrostatic adsorption with the LNPs. This surface charge facilitates the targeted delivery of the loaded mRNA to specific cells. Moreover, the LNP formulation with the prepared MC3 lipid demonstrated effective mRNA encapsulation. We then used the MC3 in preparation of LNPs with the optimized molar ratio 50:10:38.5:1.5, followed by an ethanol injection. The LNPs exhibited 79–85 nm in diameters and narrow distributions (PDI < 0.1). Literature on LNP injection shows smaller particles leave the injection site more readily compared to larger particles leading to efficient lymph node drainage and cellular interactions. The mRNA-LNPs sized 80–100 nm are preferentially taken up by antigen presenting cells (APCs), elicit antigen expression, and generate an immune response.

The cellular uptake and distribution of mRNA-LNPs are dependent on the electrostatic interaction between the positively charged head of the ionizable lipid and negatively charged mRNA (25). Furthermore, the branched tail of the lipid could facilitate mRNA release to cytosol (22, 23). Here, mRNA-LNPs exhibited lower zeta potential than un-loaded LNP, which could be attributed to the negative charge of mRNA and strong electrostatic adsorption with LNPs. This surface charge operates the loaded mRNA towards the targeted cells. Furthermore, a good mRNA encapsulation occurred in the LNP formulation with the prepared MC3 lipid. The pivotal feature of the ionizable lipids necessary for potent delivery is the pKa value because the lipid should be ionizing rapidly to release the mRNA cargo in an adequate site (26). The surface pKa values 6.44 for DLin-MC3-DMA, 6.75 for SM-102, and 6.09 for ACL-315 have been estimated (27), which means easier binding to RNA and optimal delivery. In our study, the pKa value was estimated at 6.48, which is the optimum range for intramuscular delivery of the mRNA-LNPs. These data indicate the synthesized MC3 lipid as a key component of LNP formulations could affect the intracellular delivery of mRNA. At this point, the transfection efficiency of the formulated mRNA-LNPs was monitored by using fluorescent in HEK293T cells. The kinetics of GFP expression in the mRNA-LNPs-transfected HEK293T cells showed a high transfection level indicating the success of MC3-based LNPs as a delivery vehicle. Maximizing cellular uptake and enabling an efficient release of mRNA from the endosome are key performance criteria for an LNP delivery system (23). Cationic lipids have the responsibility of driving cellular uptake and endosomal escape rendering the mRNA available in the cytosol. Despite including several cationic lipids in the composition of approved medicines, the efficient escape and cytosolic delivery of cargo, and the long tissue half-life of these lipids that lead to adverse side effects such as liver accumulation and anaphylactic shock (24, 25) remain a major challenge. Hence, efficient entrapment of LNPs at anionic membranes of endosomes to promote mRNA escape entails an ionizable lipid with increased delivery efficiency, low toxicity, and rapid in vivo metabolism characteristics. Lipids are a significant component of edible plants, serving as carriers for intercellular transport and cellular uptake. Cationic lipids derived from edible plants may have significant potential for application in this field. Given that the human immune system is adapted to edible plant stimuli, lipids of their origin are devoid of any discernible toxicity or immunogenicity, thereby promoting the LNP formulations toward low cytotoxicity. In this study, we synthesized a cationic lipid derived from safflower, analyzed the physicochemical properties necessary for mRNA delivery using LNP, and introduced an effective mRNA delivery platform with reduced cytotoxicity. The efficacy of the system should be evaluated in terms of its capacity for delivering the desired cargo to mesenchymal cells, its ability to induce an immune response, its impact on cytokine production, and its safety and tolerability in animal models.

Authors' Contribution
S.S and AM.H designed the mRNA construct, supervised the project, analyzed the data, interpreted the results, and prepared the draft of the manuscript; H.NI and AM.H performed the MC3 synthesis, conducted analysis, and formulated LNPs; S.S and S.S directed the cellular uptake experiment; Z.Sh and A.M prepared the IVT-mRNA transcript.

Ethics
This study as a non-interventional experiment is not included human or animal subjects. Safflower (*Carthamus tinctorius* L.,) seeds were used in this study kindly provided by the National Agricultural Research Institute, Isfahan, Iran.

Conflict of Interest
The authors declare that they have no conflicts of interest.

Data Availability
The authors declare that all data generated or analyzed during this study are available within the paper. Restrictions may apply to the availability of some data used under license from the funders for the current research and are not publicly available. Data are, however, available from the authors upon reasonable request and with permission from the funders.

References

1. Thi TT, Suys EJ, Lee JS, Nguyen DH, Park KD, Truong NP. Lipid-based nanoparticles in the clinic and clinical trials: from cancer nanomedicine to COVID-19 vaccines. Vaccines. 2021;9(4):359.
2. Midoux P, Pichon C. Lipid-based mRNA vaccine delivery systems. Expert Rev Vaccines. 2015;14(2):221-234.
3. Hu B, Zhong L, Weng Y, Peng L, Huang Y, Zhao Y, Liang XJ. Therapeutic siRNA: state of the art. Signal Transduct Target Ther. 2020; 5(1):101.
4. Qin S, Tang X, Chen Y, Chen K, Fan N, Xiao W, Zheng Q, Li G, Teng Y, Wu M, Song X. mRNA-based therapeutics:

powerful and versatile tools to combat diseases. Signal Transduct Target Ther. 2022;7(1):166.

5. Reichmuth AM, Oberli MA, Jaklenec A, Langer R, Blankschtein D. mRNA vaccine delivery using lipid nanoparticles. Ther Deliv. 2016;7(5):319-334.

6. Wilson B, Geetha KM. Lipid nanoparticles in the development of mRNA vaccines for COVID-19. J Drug Deliv Sci Technol. 2022;74:103553.

7. Wolff JA, Malone RW, Williams P, Chong W, Acsadi G, Jani A, Felgner PL. Direct gene transfer into mouse muscle in vivo. Science. 1990;247(4949):1465-1468.

8. Kowalski PS, Rudra A, Miao L, Anderson DG. Delivering the messenger: advances in technologies for therapeutic mRNA delivery. Mol Ther. 2019; 27(4):710-728.

9. Uchida S, Perche F, Pichon C, Cabral H. Nanomedicine-based approaches for mRNA delivery. Mol Pharm. 2020;17(10):3654-3684.

10. Andries O, Mc Cafferty S, De Smedt SC, Weiss R, Sanders NN, Kitada T. N1-methylpseudouridine-incorporated mRNA outperforms pseudouridine-incorporated mRNA by providing enhanced protein expression and reduced immunogenicity in mammalian cell lines and mice. J Control Release. 2015;217:337-344.

11. Pardi N, Hogan MJ, Porter FW, Weissman D. mRNA vaccines—a new era in vaccinology. Nat Rev Drug Disco. 2018; 17(4):261-279.

12. Eygeris Y, Gupta M, Kim J, Sahay G. Chemistry of lipid nanoparticles for RNA delivery. Acc Chem Res. 2021;55(1):2-12.

13. Carrasco MJ, Alishetty S, Alameh MG, Said H, Wright L, Paige M, Soliman O, Weissman D, Cleveland IV TE, Grishaev A, Buschmann MD. Ionization and structural properties of mRNA lipid nanoparticles influence expression in intramuscular and intravascular administration. Commun Biol. 2021;4(1):956.

14. Malburet C, Leclercq L, Cotte JF, Thiebaud J, Bazin E, Garinot M, Cottet H. Size and charge characterization of lipid nanoparticles for mRNA vaccines. Anal Chem. 2022;94(11):4677-4685.

15. Hajj KA, Ball RL, Deluty SB, Singh SR, Strelkova D, Knapp CM, Whitehead KA. Branched-tail lipid nanoparticles potently deliver mRNA in vivo due to enhanced ionization at endosomal pH. Small. 2019;15(6):1805097.

16. Zhang Y, Sun C, Wang C, Jankovic KE, Dong Y. Lipids and lipid derivatives for RNA delivery. Chem Rev. 2021; 121(20):12181-12277.

17. Rietwyk S, Peer D. Next-generation lipids in RNA interference therapeutics. ACS Nano. 2017;11(8):7572-7586.

18. Katkade MB, Syed HM, Andhale RR, Sontakke MD. Fatty acid profile and quality assessment of safflower (Carthamus tinctorius) oil. JPP. 2018;7(2): 3581-3585.

19. Shahsavandi S, Hariri AA. SARS-CoV-2 Variant-Specific mRNA Vaccine: Pros and Cons. Viral Immunol. 2023;36(3):186-202.

20. Patel R, Kaki M, Potluri VS, Kahar P, Khanna D. A comprehensive review of SARS-CoV-2 vaccines: Pfizer, moderna & Johnson & Johnson. Human Vaccin Immunother. 2022;18(1):2002083.

21. Chen L, Simpson JD, Fuchs AV, Rolfe BE, Thurecht KJ. Effects of surface charge of hyperbranched polymers on cytotoxicity, dynamic cellular uptake and localization, hemotoxicity, and pharmacokinetics in mice. Mol Pharm. 2017;14(12):4485-4497.

22. Zhang Y, Sun C, Wang C, Jankovic KE, Dong Y. Lipids and lipid derivatives for RNA delivery. Chem Rev. 2021;121(20):12181-12277.

23. Hou X, Zaks T, Langer R, Dong Y. Lipid nanoparticles for mRNA delivery. Nat Rev Mater. 2021;6(12):1078-1094.

24. Carrasco MJ, Alishetty S, Alameh MG, Said H, Wright L, Paige M, Soliman O, Weissman D, Cleveland TE 4th, Grishaev A, Buschmann MD. Ionization and structural properties of mRNA lipid nanoparticles influence expression in intramuscular and intravascular administration. Commun Biol. 2021;4(1):956.

25. Schlich M, Palomba R, Costabile G, Mizrahy S, Pannuzzo M, Peer D, Decuzzi P. Cytosolic delivery of nucleic acids: The case of ionizable lipid nanoparticles. Bioeng Transl Med. 2021;6(2):e10213.

26. Patel P, Ibrahim NM, Cheng K. The Importance of Apparent pKa in the Development of Nanoparticles Encapsulating siRNA and mRNA. Trends Pharmacol Sci. 2021;42(6):448-460.

27. Zhang C, Ma Y, Zhang J, Kuo JC, Zhang Z, Xie H, Zhu J, Liu T. Modification of lipid-based nanoparticles: an efficient delivery system for nucleic acid-based immunotherapy. Molecules. 2022;27(6):1943.